Edited by S. Selberherr, H. Stippel, E. Strasser - September 1993

Influence of Oxide-Damage on Degradation-Effects in Bipolar-Transistors

W. Bergner, B. Seidl, H. Wurzer, R. Mahnkopf, and H. Klose

Corporate Research and Development, Siemens AG
Otto-Hahn-Ring 6, D-81739 München, GERMANY

Abstract

To optimize sub-micron bipolar devices with respect to speed and stability, the precize physical mechanisms have to be understood and modeled, which describe the emitter-base breakdown itself, the charge injection into the emitter-base cap oxide and the resulting change of both forward and reverse charactersitics. The purpose of this paper is to analyze the physical effects involved, to model them and to show by comparison with measured data the accuracy of the calculated results.

1. Introduction

The device investigated is a bipolar transistor realized by a high performance 0.8 micron BICMOS process [1] (see Fig. 1 for a cross section). The 2-D doping profiles for this device were determined using the MIMAS simulation program [2] and verified by SIMS measurements in the vertical direction for both the active and inactive transistor regions. By using the device simulation program GALENE II [3], very good agreement between measured and calculated forward biased electrical characteristics was found, what indicates correct emitter/base doping profiles.

2. Stress process

A reverse bias applied between emitter and base causes leakage current due to the generation of carriers by band-to-band tunneling and impact ionization. Utilizing the device simulation program GALENE II this effect can be calculated selfconsistently [4]. A portion of the generated carriers is injected into the spacer oxide and damages the transistor. The model which describes this, weights the distance of the carriers to the oxide and their energy via the height of the oxide barrier and the thermal scattering length respectively, it has proven to be valid for MOS devices [5]:

$$j_{inj}(r_0) = \frac{A}{2\pi\lambda^2} \int_{Si} d^2r \; j(r) e^{-\frac{|r-r_0|}{\lambda}} \int_{\epsilon_b}^{\infty} f_{loc}(\epsilon, r) d\epsilon \tag{1}$$

A is a normalization constant, λ the inelastic mean free path and $j(r)$ the current density in the silicon. ϵ_b measures the energy prependicular to the interface and

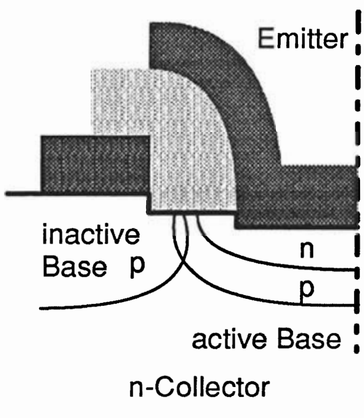

Figure 1: Schematic cross section of a bipolar transistor.

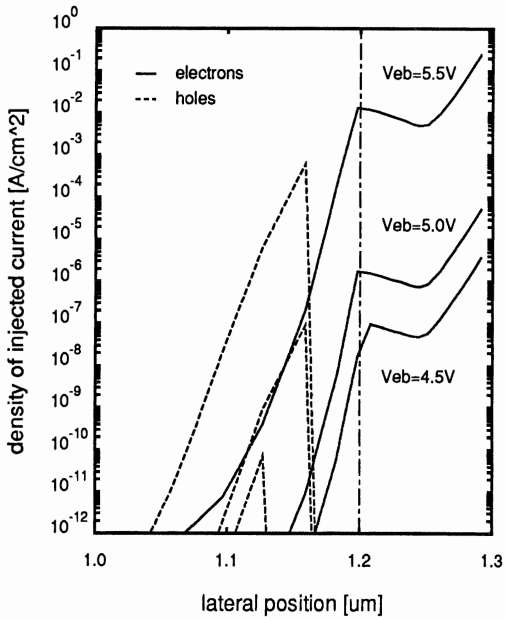

Figure 2: Calculated distribution of injected electrons and holes along the spacer for different stress voltages V_{eb}. The vertical line marks the base-emitter junction.

relative to the oxide barrier. The distribution function f_{loc} is calculated as a first approximation, from the local electric field. Figure 2 presents a calculation of this electron and hole current density passing the silicon-silicondioxide interface. Due to the field distribution under the spacer positive charge may be expected on the base and negative charge on the emitter side of the p-n junction.

Next to that we extract the distribution of the damage created in the spacer and at the spacer interface. The damage is then characterized by three quantities:

- The surface density of fixed charges q_{ss} represents the effective trapped charge in the spacer.
- The surface recombination velocity s_n and s_p results mainly from the density and capture cross section of midgap states at the interface.
- Interface traps created in the lower and upper part of the bandgap are modeled by a density increasing linearly between zero at midgap and d_d (d_a) at the valence (conduction) band edge. The charge trapped in these states is controlled by the level of the Fermi energy [6].

The absolute value of these quantities can be determined by comparing simulated results with measurements [7], as shown in the following.

3. Degradation of reverse characteristics

We attribute the pronounced dependence of the change in reverse current on the emitter-base voltage after stress to a modified field distribution due to injected charges,

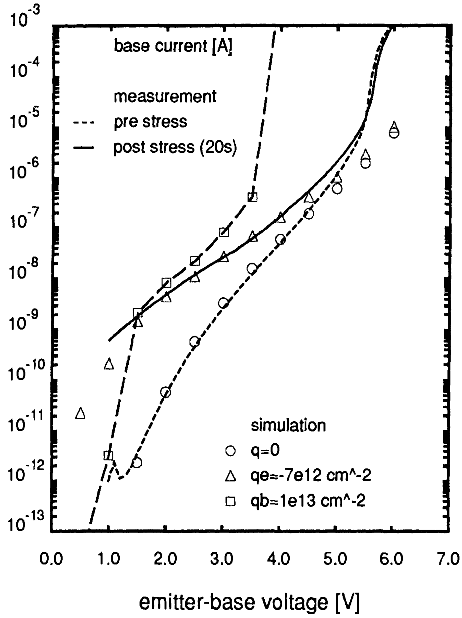

Figure 3: Comparison of measured and calculated reverse characteristics of a stressed device ($V_{eb} = 5.75V, t_{stress} = 30$s). Simulations carried out for no charge, a negative charge density at the emitter q_e and positive charge density at the base q_b.

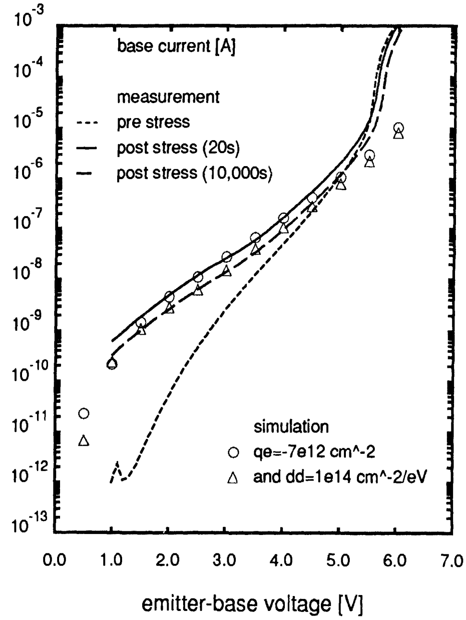

Figure 4: Comparison of measured and calculated reverse characteristics of a stressed device after $t_{stress} = 10^4$s ($V_{eb} = 5.75V$). Simulations include negative charge at the emitter q_e and donator-like interface states with a density d_d in the bandgap.

which in turn influences tunneling and avalanche currents very sensitively. Thus, we investigated this effect on the bipolar transistor. Figure 3 shows simulations for different charge configurations. The assumption of a positive charge on the base side (q_b) enhances the leakage current both in the tunneling and the avalanche branch and therefore it is inadequate for a proper description of the reverse current degradation, which shows only a small shift in the avalanche branch. In contrast to this, a negative charge located at the emitter (q_e) increases only the tunneling generation. The cause is that with increasing reverse bias the space charge exceeds the amount of injected charge and reduces its effect on the breakdown characteristics to negligible values.

It has to be noted that the increase of the leakage current is a quite fast mechanism, the tunneling current reaches a maximum after about 30s stress ($V_{eb} = 5.75V$). Further stress will reduce the tunneling by a factor of 2 within 10^4s. We attribute this to the generation of donator-like interface states at the emitter side of the junction, as reported in literature [8]. Figure 4 shows the influence of positive charged states on the leackage current, the oxide charge is compensated partially.

4. Degradation of forward characteristics

Surface states generated at the interface by injected carriers have an impact not only on the charge distribution but also on the carrier life time (increased trap density) at the interface. Both effects can be observed by analyzing the forward characteristics, because the gummel plot is sensitive to traps located in the space charge region around the p-n junction.

To describe the degradation of the forward characteristics two different kinds of recombination mechanisms have been investigated: thermal and band-to-trap tunneling recombination. Considering just the first mechanism it was not possible to describe the nonideality factor of the base current below 0.6V emitter-base voltage correctly (open circles in Fig. 5). It is quite obvious that the simulation of the forward characteristics is not independent from the reverse condition. Therefore, we have to take into account the charge distribution at the interface, which was shown to be responsible for the degradation of the reverse current. This leads us to the curve marked with the open triangles. The remaining deviation of experiment and simulation can be explained by including the enhancement of recombination by tunneling (open squares). The occupation of traps in the bandgap by tunneling causes an increased capture cross section of the traps. This can be seen at low emitter-base forward voltage as long as tunneling between the trap level and the band edge is allowed. The introduction of this effect in the simulation gives good agreement between calculation and measured data.

5. Conclusions

Within this paper it was shown that the degradation effects on the forward base current due to emitter-base reverse biasing can be explained by band-to-trap tunneling. Degradation of the breakdown characteristics after stress on the other hand results from the increasing band-to-band tunneling generation due to negative charge on the emitter side of the base-emitter junction. Thus the understanding of tunneling mechanisms is therefore neccessary to explain the generation of hot carriers and their influence on both the forward and reverse base current characteristics.

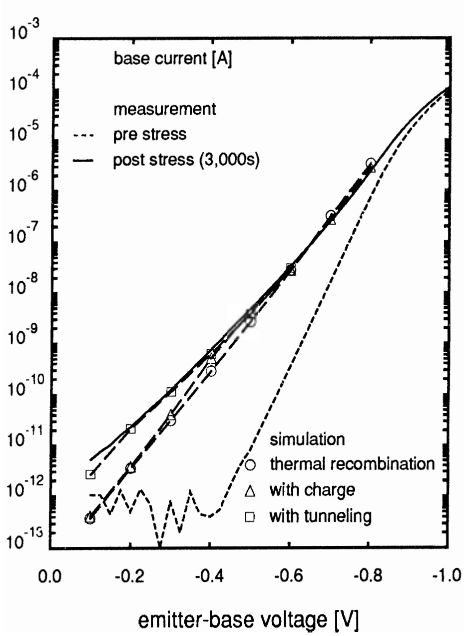

Figure 5: Comparison of measured and calculated forward characteristics of a stressed device ($V_{eb} = 5.75V$).

References

[1] H. Klose *et al.*, Proc. SSDM 1990 (1990) 653.

[2] K. Steger and M. Paffrath, Trans. IEEE CDA, to appear.

[3] GALENE II User's Guide, RWTH Aachen, Germany.

[4] W. Bergner *et al.*, Proc. ESSDERC 1992 (1992) 695.

[5] A.v. Schwerin, *et al.*, IEDM Tech. Dig., 1992.

[6] A.v. Schwerin, *et al.*, Trans. IEEE, ED-34, (1987) 2493.

[7] H. Wurzer, master's thesis, TU Munich, Germany (1992).

[8] D.A. Buchanan and D.J. DiMaria, J. Appl. Phys., 67, (1990) 7439.